Detectors and sources for ultrabroadband electro-optic sampling: Experiment and theory

A. Leitenstorfer,[a] S. Hunsche, J. Shah, M. C. Nuss, and W. H. Knox
Bell Laboratories, Lucent Technologies, 101 Crawfords Corner Road, Holmdel, New Jersey 07733

(Received 31 August 1998; accepted for publication 19 January 1999)

A detailed calculation of the amplitude and phase response of ultrathin ZnTe and GaP electro-optic sensors is presented. We demonstrate that the inclusion of the dispersion of the second-order nonlinearity is essential. Significant structures in experimental data can be explained by the theoretical response function. Correcting for the detector characteristics, we determine the precise shape of electromagnetic transients with a time resolution of 20 fs. In addition, we show that ultrafast transport of photocarriers in semiconductors can act as an efficient source for coherent electromagnetic radiation covering the entire far-to-mid-infrared regime. © *1999 American Institute of Physics.* [S0003-6951(99)02711-4]

The first amplitude and phase-sensitive detection of free-space far-infrared electromagnetic transients was demonstrated more than a decade ago.[1] Since that time, many applications of terahertz time-domain spectroscopy[2] have emerged ranging from fundamental research in condensed matter to three-dimensional imaging.[3] However, the bandwidth of this technique is limited to approximately 5 THz.[4] In recent years, an alternative detection scheme based on free-space electro-optic sampling has been developed.[5,6] Being nonresonant in nature, this approach has the potential of providing a substantially higher detection bandwidth. Indeed, sampling of electromagnetic radiation extending into the midinfrared region was demonstrated recently.[7] This frequency range is extremely interesting since it covers the vibrational resonances of molecules and solids. A comparison between photoconductive and electro-optic THz sampling can be found in Ref. 8.

In this letter, we present a calculation of the theoretical response function of electro-optic crystals which shows that inclusion of the dispersion of the second-order nonlinear coefficient is important. We also present ultrabroadband coherent measurements of free-space electromagnetic transients using extremely thin ($d \approx 10\,\mu$m) GaP and ZnTe crystals as electro-optic sensors and devices based on high-field carrier transport as emitters. Correcting the measured signals for the calculated detector response allows us to reconstruct THz wave forms with frequency content up to 70 THz.

In our experiments we employ reverse-biased GaAs and InP $p-i-n$ diodes as THz sources. The devices consist of a 5 nm semitransparent Ti contact, a 20 nm p^+ layer, and a 500 nm intrinsic zone molecular beam epitaxy grown on n^+ substrates. A convergent beam of 12 fs laser pulses with a central wavelength of 835 nm is incident on the emitter under an angle of 70°. Electron–hole pairs are excited in the intrinsic region over a large area of 1 mm by 3 mm. The average absorbed pump power in the diodes is as low as 15 mW at a pulse repetition rate of 80 MHz. The ultrafast acceleration and deceleration of the carriers in the electric field leads to the radiation of a THz electromagnetic signal into free space. This transient is detected in an electro-optic crystal at the position of the focus of the reflected pump beam at a distance of 12 mm from the diode. A gating beam is coupled in via a 500 μm Si filter with a 4 nm Au coating. The birefringence induced in the sensor by the THz electric field is sampled by the time-delayed gating pulse, which is analyzed via a shot-noise-limited detection scheme (see Refs. 5–7). As electro-optic detectors, we have studied $\langle 110 \rangle$-oriented ZnTe and GaP crystals with d between 6 and 20 μm. The sensors are contacted to inactive $\langle 100 \rangle$-oriented substrates of a thickness of 200 μm in order to prevent Fabry–Perot effects.

The complete frequency response function $R(\omega)$ of the electro-optic detectors is obtained with the following model: The influences of linear optics such as the mismatch between the THz phase velocity and the group velocity of the optical gating pulse, reflection losses at the detector surface, and absorption inside the crystal have been described recently.[6,9] The amplitude and phase of the electro-optic modulation for a given THz frequency ω is proportional to the complex function $G(\omega)$ given by Eq. (2) in Ref. 6:

$$G(\omega) = 2/[n(\omega)+1] \times \frac{c \times [\exp\{-i2\pi\omega d(n_g(\lambda_0)-n(\omega))/c\}-1]}{-i2\pi\omega d[n_g(\lambda_0)-n(\omega)]}. \quad (1)$$

The group refractive index $n_g(\lambda_0)$ at the wavelength of the optical gating pulse is calculated from dispersion data in the near-infrared regime. The dielectric response of a harmonic oscillator is used to parametrize the complex refractive index $n(\omega)$ of the THz radiation:

$$n(\omega) = \sqrt{\left[1 + \left\{\frac{(\hbar\omega_{\mathrm{LO}})^2 - (\hbar\omega_{\mathrm{TO}})^2}{(\hbar\omega_{\mathrm{TO}})^2 - (\hbar\omega)^2 - i\hbar\gamma\omega}\right\}\right] \times \epsilon_\infty}. \quad (2)$$

The absolute value of $G(\omega)$ calculated for a GaP detector of a thickness $d = 13\,\mu$m is depicted versus frequency in Fig. 1(a). A structured dip in the amplitude spectrum appears in the reststrahl region around 11 THz. This feature reflects

[a]Electronic mail: aleitens@physik.tu-muenchen.de

 © 1999 American Institute of Physics
Downloaded 22 Feb 2002 to 128.113.8.139. Redistribution subject to AIP license or copyright, see http://ojps.aip.org/aplo/aplcr.jsp

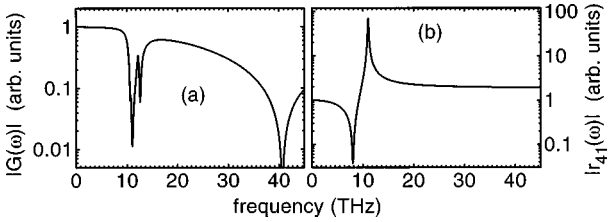

FIG. 1. Amplitude of the linear part of the detector response function $G(\omega)$ vs frequency (a) and dispersion of the absolute value of the electro-optic coefficient $r_{41}(\omega)$ (b) as calculated for a GaP electro-optic sensor of a thickness of 13 μm.

the high absorption of the material and the large velocity mismatch near the lattice resonance. Above 20 THz, the amplitude of $G(\omega)$ rolls off since the accumulated time delay between the gating pulse and the midinfrared phase approaches the inverse frequency of the THz radiation. At 40 THz, the probe pulse sweeps over exactly one THz cycle while passing through the crystal resulting in a cancellation of the polarization rotation.

$G(\omega)$ represents the detector response only if the electro-optic coefficient r_{41} of the sensor material is frequency independent. However, r_{41} exhibits a strong dispersion and resonant enhancement due to the lattice resonance. We find that this effect accounts for very pronounced features in the response functions. An analytic expression for $r_{41}(\omega)$ has been derived in Ref. 10, Eq. (5):

$$r_{41}(\omega)=r_e\times\left[1+C\left(1-\frac{(\hbar\omega)^2-i\hbar\omega\gamma}{(\hbar\omega_{\mathrm{TO}})^2}\right)^{-1}\right]. \tag{3}$$

The Faust–Henry coefficient C represents the ratio between the ionic and the electronic part of the electro-optic effect at $\omega=0$. A negative sign of C (see Table I) indicates that both contributions subtract from each other in the frequency regime below the lattice resonance.[10,16] The purely electronic nonlinearity r_e is assumed to be constant at the mid- and far-infrared frequencies ω.

The calculated amplitude spectrum of $r_{41}(\omega)$ is shown in Fig. 1(b): The minimum at 8 THz results from a cancellation of the electronic and the lattice contributions to the optical nonlinearity. At the TO phonon frequency (11 THz in GaP), the nonlinear coefficient is resonantly enhanced. $r_{41}(\omega)$ remains high in the entire midinfrared because the electron and phonon contributions are of identical sign.

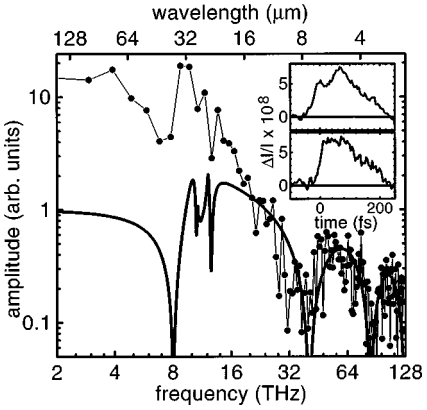

FIG. 2. Amplitude spectrum of the measured electro-optic THz signal emitted by a GaAs $p-i-n$ diode with a bias field of 130 kV/cm vs frequency (dots connected with the thin line). The thick line shows the calculated amplitude of the full response function $R(\omega)=G(\omega)\times r_{41}(\omega)$ of the 13 μm thin GaP detector. Note the logarithmic scales. In the upper inset, the uncorrected time trace of the electro-optic signal from the diode at an electric field of 30 kV/cm is displayed. The lower inset shows the original transient obtained by correcting for the detector response.

The full complex response function $R(\omega)$ of the detector is then given by

$$R(\omega)=G(\omega)\times r_{41}(\omega). \tag{4}$$

The material parameters entering our calculations of $R(\omega)$ are collected in Table I.[11–16]

Figure 2 displays the amplitude spectrum versus frequency of the THz transient from a GaAs $p-i-n$ diode as measured with a GaP sensor of a thickness $d=13\,\mu$m (dots and thin line). The bias electric field in the emitter is 130 kV/cm. For comparison, the calculated amplitude response $|R(\omega)|$ of the sensor, normalized to unity at low frequencies, is shown as a thick line in Fig. 2. The total amplitude response of the detector is flat up to a frequency of 6 THz. As expected from the dispersion of $r_{41}(\omega)$, a dip at 8 THz appears in the experimental data. Interestingly, the structure around the lattice resonance at 11 THz is not very pronounced in both the measured spectrum and the calculated $|R(\omega)|$: The minimum in $|G(\omega)|$ and the resonant enhancement of $r_{41}(\omega)$ roughly compensate for each other. The dip due to the velocity mismatch at 40 THz is also found in the measurement. Some amplitude is regained for frequencies around 60 THz before the phase delay approaches two infrared cycles at 80 THz. The higher signal amplitude in the

TABLE I. Material constants used in the calculation of the frequency response functions $R(\omega)$ of ZnTe and GaP electro-optic detectors. The transverse and longitudinal optical phonon energies and the lattice damping are denoted by $\hbar\omega_{\mathrm{TO}}$, $\hbar\omega_{\mathrm{LO}}$, and γ, respectively. ϵ_∞ is the high-frequency dielectric constant, C the Faust–Henry coefficient, and n_g the group refractive index at a wavelength of 835 nm.

	$\hbar\omega_{\mathrm{TO}}$ (cm^{-1})	$\hbar\omega_{\mathrm{LO}}$ (cm^{-1})	γ (cm^{-1})	ϵ_∞	C	n_g at 835 nm
ZnTe	177[a]	206[a]	3.01[a]	6.7[a]	$-0.07^{+0.02}_{-0.05}$[b]	3.224[c]
GaP	367.3[d]	403.0[d]	4.3[e]	9.075[f]	−0.47[g]	3.556[f]

[a]Reference 11.
[b]Value inferred by the present work.
[c]Reference 12.
[d]Reference 13.
[e]Reference 14.
[f]Reference 15.
[g]Reference 16.

Downloaded 22 Feb 2002 to 128.113.8.139. Redistribution subject to AIP license or copyright, see http://ojps.aip.org/aplo/aplcr.jsp

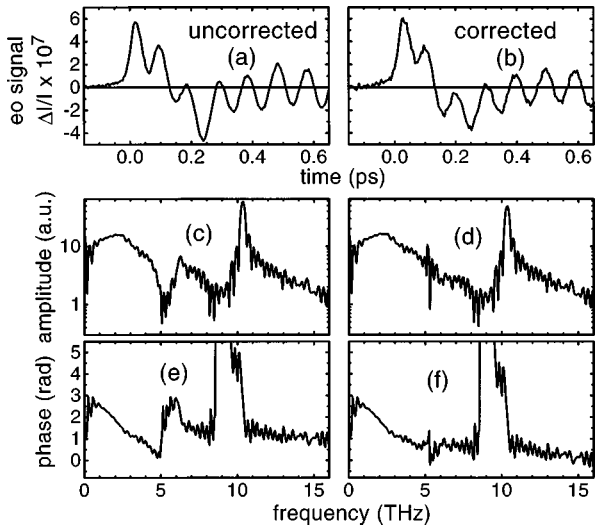

FIG. 3. (a), (c), and (e): electro-optic THz signal, amplitude, and phase spectrum from an InP emitter at a bias field of 90 kV/cm, as measured with a 8 μm thin ZnTe sensor. The corresponding data after correction for the detector response are displayed in (b), (d), and (f).

experimental spectrum at lower frequencies and some additional structures are related to the ultrafast carrier transport in GaAs,[17] which acts as a coherent source for the THz radiation. We observe frequency components up to approximately 70 THz, corresponding to a wavelength of 4 μm, which are clearly above the noise floor. To our knowledge, these results represent the highest bandwidth for amplitude and phase-resolved detection of electromagnetic radiation reported to date. This finding demonstrates that the high-field acceleration of photocarriers in biased semiconductors can be exploited as an efficient source of radiation covering the entire midinfrared regime while requiring much lower intensities and power levels than optical rectification.[7]

The early part of the measured electro-optic signal from the GaAs emitter at a bias field of 30 kV/cm is shown in the upper inset of Fig. 2: The time trace exhibits a double-step structure with two peaks separated by 80 fs. These data have been corrected for the amplitude and phase response of the sensor calculated with the model described above. The resulting signal shape is displayed in the lower inset of Fig. 2. As expected from the instantaneous onset of charge acceleration in the GaAs diode, the recovered signal exhibits a sharp rise within the 20 fs time resolution of our setup, resembling an electromagnetic shock wave. The amplitude remains constant for approximately 100 fs, indicating ballistic acceleration of the electrons in the $p-i-n$ device. A more detailed interpretation of these results is given elsewhere.[17]

In Fig. 3, the time trace of the electro-optic signal from an InP emitter diode at a bias field of 90 kV/cm is shown together with the corresponding amplitude and phase spectra. The uncorrected data are displayed on the left-hand side of Fig. 3. The data on the right-hand side have been corrected for the calculated response function of the $d=8$ μm ZnTe sensor. In contrast to the GaP detector, the dip in the amplitude spectrum [Fig. 3(c)] around the lattice resonance (5.3 THz) is much more pronounced in ZnTe. This finding indicates a weaker ionic contribution to the second-order nonlinearity in this material. The result is a smaller resonant enhancement of $r_{41}(\omega)$ in the reststrahlen band, and thus, a strongly reduced sensitivity due to reflection losses and velocity mismatch. No direct measurements of the Faust–Henry coefficient C are available for ZnTe. A theoretical study predicts a value of $C=-0.32$,[18] i.e., conditions similar to GaP where $C=-0.47$ (see Fig. 5 in Ref. 16). However, a much better fit to our experimental data is obtained if we assume a different value of $C=-0.07^{+0.02}_{-0.05}$. The origin of this discrepancy is not clear at present and further investigations are desirable. After dividing the amplitude spectrum of the experimental data [Fig. 3(c)] by $|R(\omega)|$ calculated with the ZnTe parameters given in Table I, the dip around 5.5 THz vanishes exactly [Fig. 3(d)]. Adding the argument of $R(\omega)$ to the phase spectrum compensates for the dispersive feature in the reststrahl region of ZnTe [Fig. 3(e)] and a flat phase is obtained between 3 and 16 THz [Fig. 3(f)]. The pronounced structure in the spectra around 10 THz and the harmonic oscillations in the time traces [Figs. 3(a) and 3(b)] are connected to the excitation of coherent phonons in the InP emitter material.[17]

In conclusion, we have given a full theoretical description of the response of ultrabroadband electro-optic sensors. The calculations show the importance of properly accounting for the dispersion of the electro-optic coefficient and provide excellent agreement with experimental data. As an application, the measurement of the precise time trace of midinfrared electromagnetic transients has been demonstrated. The coherent emission of Hertzian dipole radiation based on ultrafast carrier transport in semiconductors is shown to contain a frequency spectrum with components between 100 GHz and 70 THz, corresponding to the wavelength interval from 3 mm to 4 μm.

This work was partially supported by the NEDO Femtosecond Technology Project.

[1] P. R. Smith, D. H. Auston, and M. C. Nuss, IEEE J. Quantum Electron. **QE-24**, 255 (1988).
[2] For a recent overview, see M. C. Nuss and J. Orenstein, in *Millimeter-Wave Spectroscopy of Solids*, Springer Topics in Applied Physics, Vol. 74, edited by G. Gruner (Springer, Berlin, 1998).
[3] D. M. Mittleman, S. Hunsche, L. Boivin, and M. C. Nuss, Opt. Lett. **22**, 904 (1997).
[4] S. E. Ralph and D. Grischkowsky, Appl. Phys. Lett. **60**, 1070 (1992).
[5] Q. Wu and X.-C. Zhang, Appl. Phys. Lett. **68**, 1604 (1996).
[6] Q. Wu and X.-C. Zhang, Appl. Phys. Lett. **70**, 1784 (1997).
[7] Q. Wu and X.-C. Zhang, Appl. Phys. Lett. **71**, 1285 (1997).
[8] S.-G. Park, M. R. Melloch, and A. M. Weiner, Appl. Phys. Lett. **73**, 3184 (1998).
[9] H. J. Bakker, G. C. Cho, H. Kurz, Q. Wu, and X.-C. Zhang, J. Opt. Soc. Am. B **15**, 1795 (1998).
[10] W. L. Faust and C. H. Henry, Phys. Rev. Lett. **17**, 1265 (1966).
[11] A. Manabe, A. Mitsuishi, and H. Yoshinga, Jpn. J. Appl. Phys. **6**, 593 (1967).
[12] D. T. F. Marple, J. Appl. Phys. **35**, 539 (1964).
[13] A. Mooradian and G. B. Wright, Solid State Commun. **4**, 431 (1966).
[14] B. A. Weinstein and G. S. Piermarini, Phys. Rev. B **12**, 1172 (1975).
[15] A. N. Pikhtin, V. T. Prokopenko, and A. D. Yas'kov, Sov. Phys. Semicond. **10**, 1224 (1976).
[16] W. L. Faust, C. H. Henry, and R. H. Eick, Phys. Rev. **173**, 781 (1968).
[17] A. Leitenstorfer, S. Hunsche, J. Shah, M. C. Nuss, and W. H. Knox (unpublished).
[18] C.-C. Shih and A. Yariv, J. Phys. C **15**, 835 (1982).

Downloaded 22 Feb 2002 to 128.113.8.139. Redistribution subject to AIP license or copyright, see http://ojps.aip.org/aplo/aplcr.jsp